Journal of Engineering and Technology
DergiPark
AKADEMİK

Journal of Engineering and Technology 3;1 (2019) 12-24

Investigation of the effect of stator and rotor pole ratios on torque and efficiency in Inverted Switched Reluctance Motor

Ahmet YILDIZ [1*], Mehmet POLAT [1]

[1] Department of Mechatronics Engineering, Faculty of Engineering, Firat University, Elazig, Turkey

ARTICLE INFO

Article history:
Received 12 Dec 2018
Received in revised form 3 April 2019
Accepted 6 May 2019
Available online 23 May 2019

Keywords:
Switched Reluctance Motor
Stator pole ratio coefficient
Rotor pole ratio coefficient
Torque and efficiency

* Corresponding author.
E-mail address: ayildiz@firat.edu.tr

ABSTRACT

In this study, the effect of rotor pole ratio coefficient and stator pole ratio coefficient on torque and efficiency in 18/12 pole 3 phase Inverted Switched Reluctance Motor have been investigated. For this purpose, dimension, electrical and magnetic parameters of 18/12 pole 3-phase Inverted Switched Reluctance Motor have been determined. These parameters were obtained in our previous study by the heuristic optimization method according to the determined motor characteristics (efficiency, torque, etc.). The other dimensions of motor have been kept constant and the effect of rotor pole ratio coefficient and stator pole ratio coefficient on the torque and efficiency have been determined according to the fixed and calculated total ampere-turns values. As a result of the analyzes performed in MATLAB, it has been observed that there have certain relationships between these coefficients and torque-efficiency. However, since the effects of rotor pole ratio coefficient and stator pole ratio coefficient on torque and efficiency are not exactly linear, it can seen that these coefficients will be considered as optimization problems in future studies and optimization of these coefficients will be beneficial in terms of motor performance.

1. Introduction

The Switched Reluctance Motor (SRM) is a simple-structured electric machine consisting of stator and rotor salient poles and without winding in the rotor. SRMs are converts mechanical energy to electrical energy with reluctance force. The difference of Inverted Switched Reluctance Motors (ISRM) from SRMs is the change of rotor and stator places. All the operating features of ISRMs are exactly the same as a normal SRM.The ability to produce a continuous torque depends on the position of the rotor pole relative to the stator pole and the suitable phase windings being fed respectively. A power electronics circuit and control mechanism are also required to supply this. Although SRMs were introduced as a principle in the 1800s, it was possible to drive the motor in the early 1960s due to the developments in power electronics. Especially the studies on this motor have been concentrated after 1980. In recent years, significant developments have been achieved in SRMs. In parallel with the developments in software, design and technology, the reason for tending to SRM is that the structure of these motors is simple, reliable and stable, almost independent from the working environment, can be operated at low and high speeds [1-3]. In addition, the cost of production and maintenance-repair costs are low [4-5].

SRMs are widely used in automobile, railway, aviation and marine industries, electrical household appliances, fans, pumps and elevators [6-8].

In order to rotate the SRM, the number of stator and rotor poles are different. If high speed is desired from the SRMs, the number of rotor poles must be smaller than number of stator poles, and if the high torque is desired, the number of rotor poles is selected to be close to the number of stator poles. Stator and rotor pole combinations used in SRMs are shown in Table 1 [9-10].

Table 1. Pole combinations and the corresponding number of phases

Ns/Nr	6/4	6/8	12/8	18/12	8/6	8/10	16/12	24/18	10/6	10/12	12/10	14/12
Number of phases	3	3	3	3	4	4	4	4	5	5	6	7

SRMs can be produced in different phase numbers starting from a phase. However, 3 and 4 phase SRMs are widely produced for commercial. In Figure 1, one, two, three and four phase SRM types are shown. The structure of one-phase SRMs is very simple, the machine with the least connection between the drive circuit and the motor. Although they are attractive for very high speed applications, these motors cannot run by themselves, and they have more vortex losses. This type of motors 2/2 and 4/4 poles can be made but in this case, the produced torque is very ripple [11]. The problem of running in two-phase SRMs was overcome by an asymmetric structure in the rotor poles. But the ripple in the torque is still high. Three-phase SRMs are generally made of 6/4 and 12/8 poles. They have a high starting torque. In these motors, the ripple in the torque is decreasing but continues. Four-phase SRMs are made of 8/6-pole and five-phase SRMs are made of 10/8 poles, and are recommended to reduce the torque ripple. However, the number of connections between the driver circuit and the motor increases as more power electronics are used [12-13].

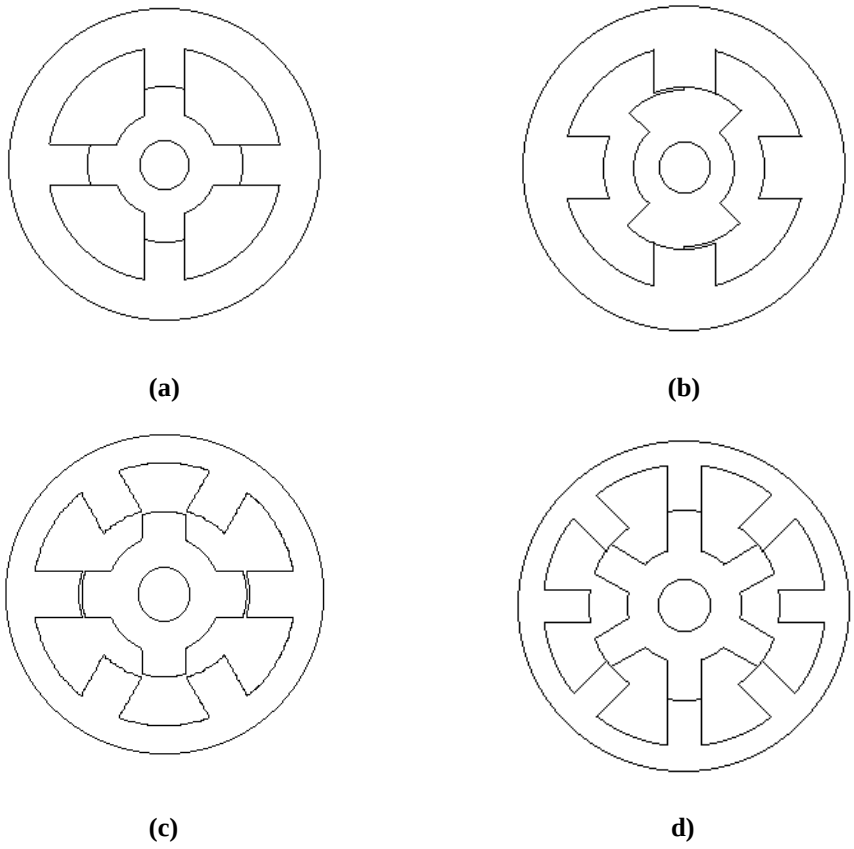

Figure 1. SRM types according to stator and rotor poles number

a) One-phase 4/4 pole SRM, b) Two-phase 4/2 pole SRM, c) Three-phase 6/4-pole SRM, d) Four-phase 8/6-pole SRM

SRMs has basically two problems. The first is the acoustic noise caused by the torque ripple and radial forces when SRM is operating. The other is the determination of the motor position. The forces in the direction of the radius and acting on the rotor poles cause vibrations in the bearings. These vibrations are perceived as acoustic noise in the stator. These vibrations to the bearings can cause the bearings to malfunction after a period of time. Vibration and acoustic noise can be reduced thanks to innovations in control systems and motor design.

SRMs are very advantageous compared to other AC and DC motors because of their simple and robust structure, high torque to weight ratio and high fault tolerance [14-16]. In SRMs, there are only windings in the stator and no windings in the rotor and the absence of magnets in the structures make these motors advantageous in terms of cost and production. In addition, the high power output of the motors in SRMs is a powerful alternative to AC and DC motors, especially due to the high efficiency and cost advantages of the system [17]. Table 2 shows the comparison of SRM with other motors.

Table 2. The comparison of SRM with other motors

	Induction Motor	**Synchronous Motor**	**DC Motor**	**Step Motor**	**SRM**
Supply voltage	Alternating voltage	Alternating voltage	Direct voltage	Direct voltage	Direct voltage
Excitation voltage	Not required	Direct voltage	Direct voltage	Not required	Not required
Driver	Necessary in variable speed applications	Necessary in variable speed applications	Necessary in variable speed applications	Always necessary	Always necessary
Operation and maintenance costs	Low	Low	Average	Low	Low
Cost	Low	High	Average	Average	Average
Driver cost	High	High	Average	Average	High
Efficiency	High	High	Average	Average	High

In SRM design, rotor and stator pole numbers, pole width, pole arcs are directly effective on motor performance. There are many studies on these parameters in literature. Choi et al. proposed a new stator pole face with an irregular air gap profile and a pole shoe attached to the lateral face of the rotor pole to reduce unwanted torque ripple of a Switched Reluctance Motor. The effects of the design parameters were simulated using the finite element method and optimized by applying the response surface methodology (RSM). By optimizing the pole shoe and the air gap profile, the torque wave was reduced to 23% of its value before optimization [18]. Arumugam et al. investigated the effect of the pole arc / pole pitch ratio of the rotor and stator on the performance of a Switched Reluctance Motor. They used an analytical method based on two-dimensional finite element analysis and magnetic flux path. They indicated that the range of values that could be used for the pole arc/ pole pitch ratio of the rotor could be between 0.3 to 0.45 and the stator could be between 0.35 and 0.5 [19]. Gungor and Uygun have tried to find out an easy way to determine the suitable and acceptable ratio between the stator and rotor tooth width in the Switched Reluctance Motors for torque and output power, smoother magnetic field energy. In order to find the most appropriate ratio, they did 8 different SRM designs and used the finite element method analysis [20].

In this study, the effects of rotor and stator pole ratio coefficients on torque and efficiency in ISRM have been investigated. For this purpose, the electrical and dimensional parameters of ISRM have been calculated in MATLAB considering the non-linearity of the motor. Then, the results for fixed and variable cases of total amperes have been examined.

2. Material And Method

In this study, firstly, dimension, electrical and magnetic parameters of 18/12 pole 3-phase ISRM have been determined. These parameters were obtained in [21] by the heuristic optimization method according to the determined motor characteristics (efficiency, torque, etc.). In the next step, the other dimension parameters of the ISRM were kept constant and the effect of C_{spr} and C_{rpr} coefficients on the torque and efficiency was examined according to the fixed and calculated TAT values. The equations that symbolize the coefficients are given in Equation (1-2). The parameters in the equations are shown in Figure 2. In order for this study to be realistic, it has been checked whether the number of windings per phase obtained will be fitted into in stator slots. Winding results that could not be fit in the slots were eliminated.

Rotor ratio coefficient (C_{rpr}) is

$$C_{rpr} = \frac{C}{C + h_r} \tag{1}$$

Stator ratio coefficient (C_{spr}) is

$$C_{spr} = \frac{C_{in}}{C_{in} + h_s} \tag{2}$$

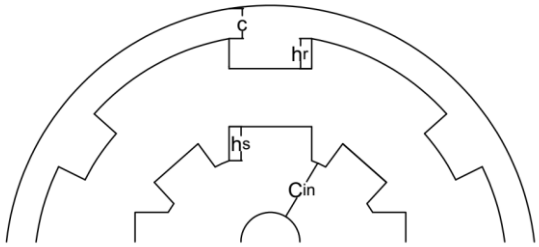

Figure 2. Dimension parameters of ISRM

2.1 Torque Generation in Switched Reluctance Motor

In SRM, the torque generation is based on the conversion of magnetic energy to mechanical energy by taking advantage of the reluctance change between the unaligned position and the aligned position. As shown in Figure 3, when a phase in the SRM is excitation, positive torque is generated positive where the inductance slope is positive, zero in the region where it is fixed, and finally negative torque generated where the slope is negative.

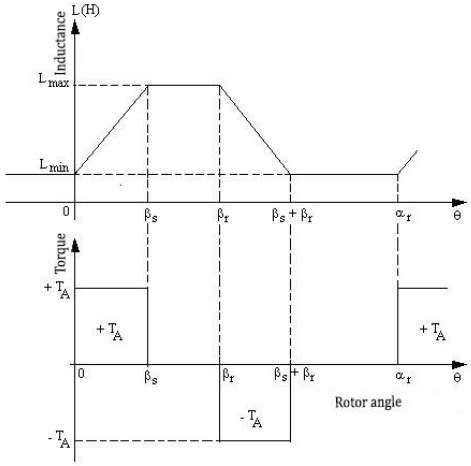

Figure 3. Variation of the torque generated in SRM due to inductance of a phase

Instantaneous torque in any phase i [22];

$$T_i = \frac{1}{2} i_i^2 \frac{\partial L_i(\theta)}{d\theta} \tag{3}$$

can be calculated by relation. By using the inductance curve in Figure 3 with the expression in Equation (3), the mathematical torque relations in Equation (4) for phase A can be derivation [9]:

$$T_a = \begin{cases} \frac{1}{2} K i_a^2 & 0 \le \theta \le \beta_s \\ 0 & \beta_s \le \theta \le \beta_r \\ -\frac{1}{2} K i_a^2 & \beta_s \le \theta \le \beta_s + \beta_r \\ 0 & \beta_s + \beta_r \le \theta \le \alpha_r \end{cases} \tag{4}$$

The total torque developed by the motor is equal to the sum of the instantaneous torques generated by the individual phases.

$$T_e(\theta, i_a, \dots, i_d) = \sum_{i=1}^{q} T_i = \frac{1}{2} \sum_{i=1}^{q} i_i^2 \frac{\partial L_i(\theta)}{d\theta} \tag{5}$$

In order to ensure that the instantaneous motor torque is not zero at any rotor position, the β_s must be greater than α_r/q.

2.2 Deriving Equations of ISRM Dimension and Electrical Parameters

The electrical and dimensional parameters of the ISRM are calculated using Equations (6-25) via MATLAB. The dimension parameters in the equations are shown in Figure 4. In addition, the B-H characterization of the silicone sheet should be taken into account when the nonlinear equations of the ISRM are derived. The B-H characteristic of the silicon sheet is shown in Figure 5. In the ISRM design, the magnetic induction density must not exceed the knee point in nominal operating conditions.

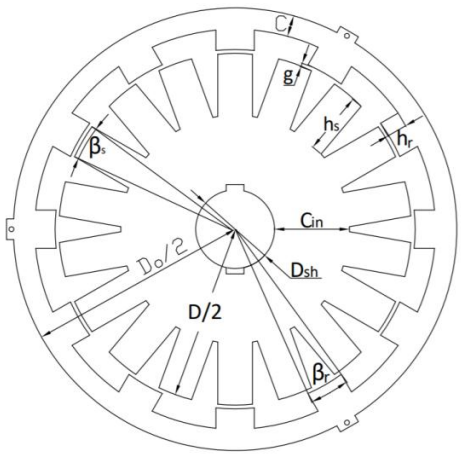

Figure 4. Dimension parameters of ISRM

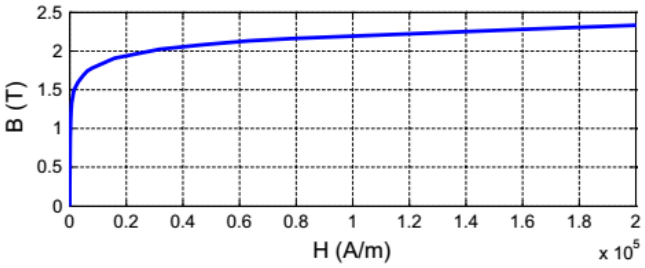

Figure 5. B-H Characteristic of silicone sheet

The flux density of stator pole (B_s) is assumed as equal to B_{max}. Omitting leakage flux and packaging factor, stator pole area (A_s) is estimated as [21];

$$A_s = \left(\frac{D}{2} - g\right) \cdot L \cdot \beta_s \tag{6}$$

where L refers to package length of motor.
Flux in stator pole is

$$\emptyset = B_s \cdot A_s \tag{7}$$

Flux in yoke is

$$\emptyset_y = \frac{\emptyset}{2} = \frac{B_s \cdot A_s}{2} \tag{8}$$

Area of yoke is

$$A_y = C_{in} \cdot L \tag{9}$$

Flux density of yoke is

$$B_y = \frac{Q_y}{A_y} \tag{10}$$

Length of stator pole is

$$h_s = \left(\frac{D}{2} - g - \frac{D_{sh}}{2}\right) - \frac{A_y}{L} \tag{11}$$

Length of rotor pole is

$$h_r = \frac{D_0}{2} - C - \frac{D}{2} \tag{12}$$

Magnetic field intensity in air gap is calculated by

$$H_g = \frac{B_g}{4 \cdot \pi \cdot 10^{-7}} \tag{13}$$

B-H curve is determined as a function then magnetic field density values corresponding to B_s, B_g, B_r, and B_{rc} are obtained by this function. Consequently, the flux path equations are estimated. Thus, path length of rotor region is

$$l_r = h_r + \frac{C}{2} \tag{14}$$

Path length of rotor yoke is

$$l_{ry} = (2 \cdot \pi \cdot NP \cdot 0.5 \cdot (D_0 - C))/N_s \tag{15}$$

Path length of air gap region is

$$l_g = g \tag{16}$$

Path length of stator region is

$$A_s = \left(\frac{D}{2} - g\right) \cdot L \cdot \beta_s \tag{17}$$

Path length of stator core is

$$l_s = (0.25 \cdot D - 0.5 \cdot g + 0.5 \cdot h_s - 0.25 \cdot D_{sh}) \tag{18}$$

In this situation, total ampere-turns (TAT) can be calculated as

$$TAT = 2 \cdot (H_s \cdot l_s + H_r \cdot l_r) + \left(B_g \cdot \frac{A_g}{P_a}\right) + (H_{ry} \cdot l_{ry} + H_{sy} \cdot l_{sy}) \tag{19}$$

where P_a refers to permeability.
Turn per phase is

$$T_{ph} = \frac{TAT}{I_p} \tag{20}$$

where I_p refers to rated current.

Current rate is

$$i_p = \frac{TAT}{T_{ph}} \tag{21}$$

Accurate estimation of inductances, L_a and L_u is crucial for reliable design. High estimation error of inductances causes the torque to be calculated wrong. Therefore, to calculate the inductances (L_a and L_u) at aligned and unaligned positions, respectively 2 base and 7 base flux-paths are selected. The rest of the fluxes can cause raising the estimation complexity and variation of the result will be trivial, as shown in Figure 6 and Figure 7.

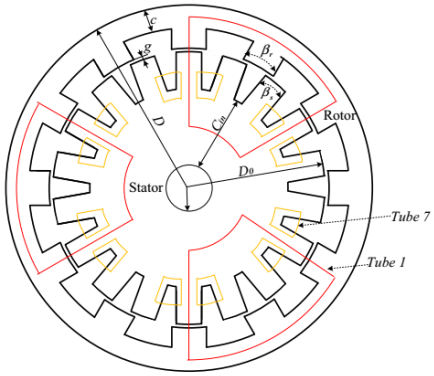

Figure 6. Flux paths for inductance calculation of ISRM at aligned position (La) [21].

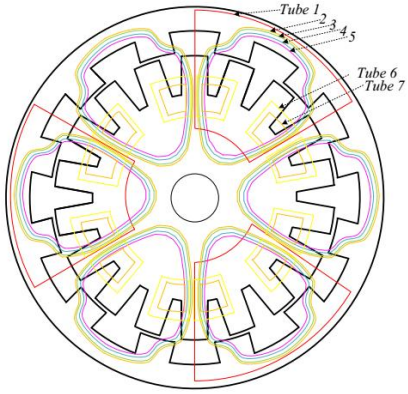

Figure 7. Flux paths for inductance calculation of ISRM at unaligned position (Lu) [21].

The inductance values obtained by using the flux paths are transferred to the energy calculation. Energy calculation at aligned and unaligned position, average torque of pole pair, and average torque are all respectively given as;

$$W_a = \frac{1}{2} \cdot L_a \cdot {i_p}^2 \tag{22}$$

$$W_u = \frac{1}{2} \cdot L_u \cdot {i_p}^2 \tag{23}$$

$$T_{pp} = \frac{((W_a - W_u) \cdot N_s \cdot N_r)}{N_{tpp} \cdot \pi} \tag{24}$$

$$T_{average} = T_{pp} \cdot N_{tpp} \cdot 0.5 \tag{25}$$

3. Results and Discussion

In the first case, TAT value calculated from Equation (19) has not been calculated and it has been taken constant at different intervals from 4000 AT to 6000 AT and torque and efficiency changes were examined according to C_{spr} and C_{rpr} values. Figures 8a and 8b show the effect of C_{spr} and C_{rpr} ratios on the generated torque. As it is seen in the figure as the C_{spr} ratio increased, the torque increased but the torque decreased as the C_{rpr} ratio increased. In addition, when Figure 8a is carefully examined, the torque is not calculated at 5000 AT and above values because the windings do not fit into the slots with these C_{spr} values.

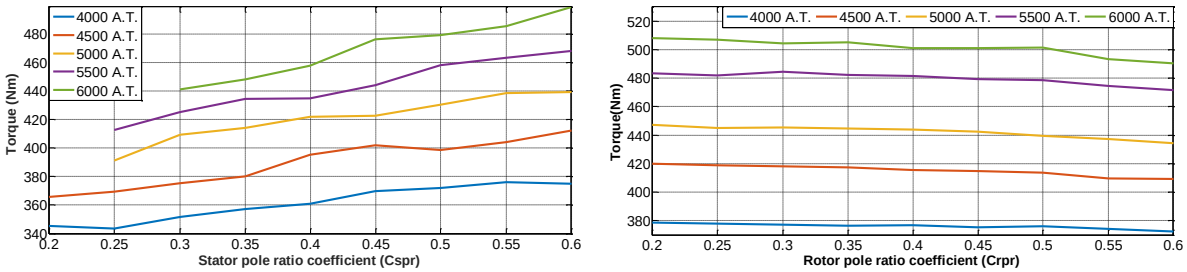

(a) (b)

Figure 8. Torque vs pole ratio coefficients for different ampere-turns

Figures 9a and 9b show the effects of C_{spr} and C_{rpr} values on efficiency of ISRM. It has been observed that the increase C_{spr} ratio had a negative effect on efficiency, but C_{rpr} had no effect on efficiency because the total ampere- turns did not change and only copper losses were examined in this study.

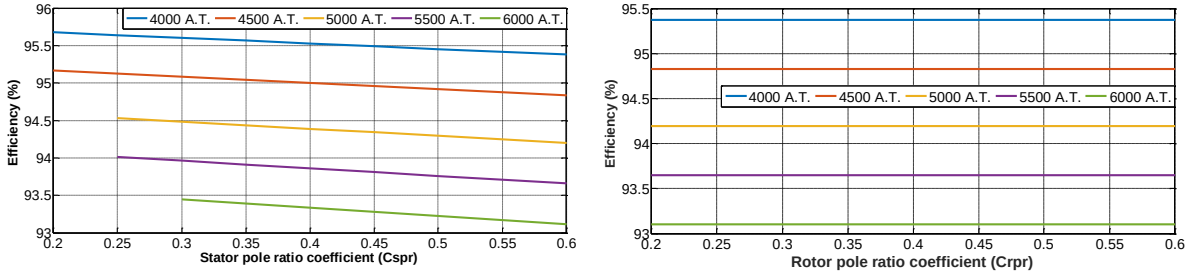

(a) (b)

Figure 9. Efficiency vs pole ratio coefficients for different ampere-turns

Figures 10 and 11 show the three-dimensional figures of the effects of C_{spr} and C_{rpr} in the nominal current (75A) on the torque and efficiency, respectively. When Figure 10 is examined, it is observed that high torque can be obtained at high values of C_{spr} and low values of C_{rpr}. Figure 11 shows that lower C_{spr} values are required for higher efficiency. The higher values of C_{rpr} increase the torque while the lower values increase the efficiency. It is necessary to pay attention to this case and the most appropriate value should be selected according to the desired case.

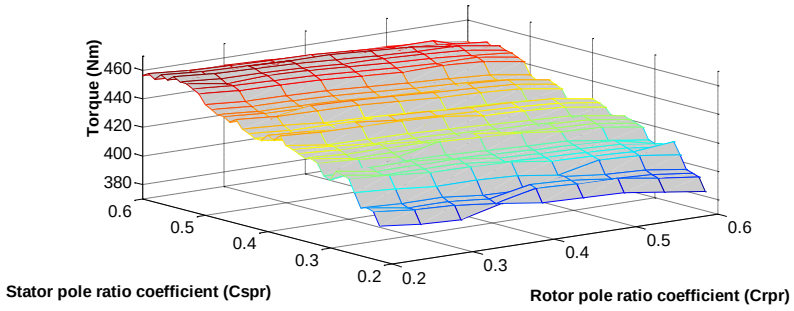

Figure 10. Torque vs pole ratio coefficients

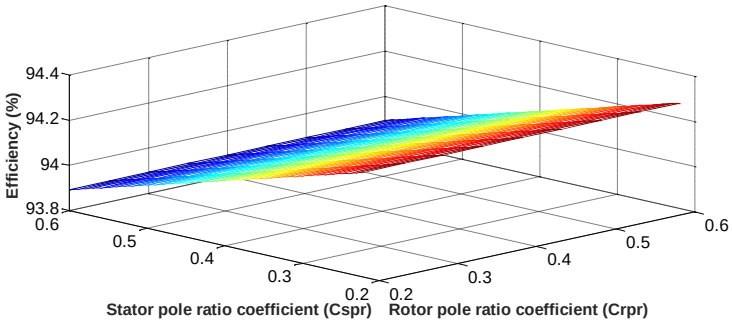

Figure 11. Efficiency vs pole ratio coefficients

In the second case, the effect of C_{spr} and C_{rpr} ratios on the torque and efficiency was investigated by taking into account the Equation (19) in different current values (60-100 A). In Figures 12a and 12b, the effect of C_{spr} and C_{rpr} ratios on the torque is shown. Since the torque values in both figures follow the same curve, the torque in each current value was plotted by multiplying 0.01 times according to the previous figure ($a=1$ $Tort=Tort*a$, $a=a+0.01$). In this way, the figures can be made clearer and interpreted. When Figure 8a is examined, it is observed that there is no complete linearity between C_{spr} ratio and torque. As the C_{spr} coefficient increased until about 0.55, it was observed that the torque value increased as in Figure 4a. However, a negative effect was observed in the torque after 0.55 value of C_{spr}. It should also be considered that the number of windings calculated in some current values cannot be fitted in the stator pole slots. For example, torque generation started from 0.45 values of C_{spr} for Ip=60A and started at 0.3 for Ip = 80A. In Figure 12b, it has been observed that the ISRM starts to generate torque after 0.44 value of C_{rpr} and the torque decreased as the ratio increased as in Figure 8b.

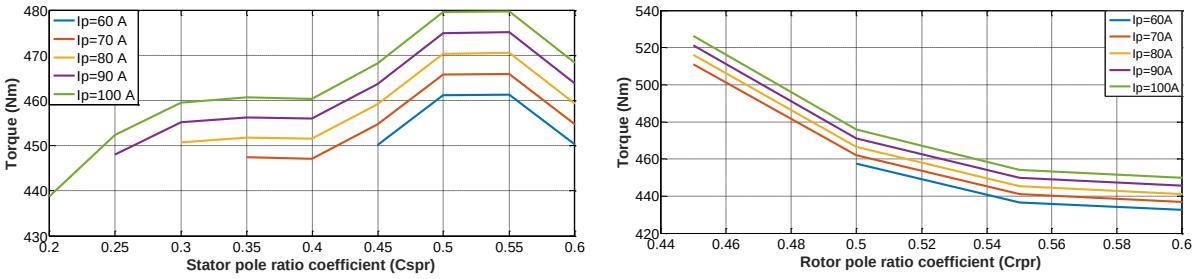

(a) (b)

Figure 12. Torque versus pole ratio coefficients for diffirent currents

Figures 13a and 13b show the effect of C_{spr} and C_{rpr} on efficiency of ISRM. Both naturally have the same values as C_{spr} and C_{rpr} in Figures 12a and 12b (horizontal axis is the same). As is also observed from the figures, the efficiency increased as the ratio increased in both. These results were observed to be completely opposite to the fixed TATs. However, it should not be forgotten that only copper losses are investigated in this study.

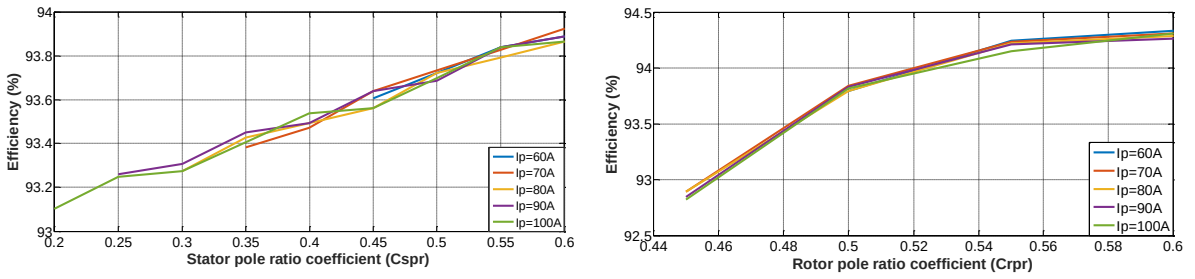

(a) (b)

Figure 13. Efficiency versus pole ratio coefficients for diffirent currents

Figures 14 and 15 show the three-dimensional figures of the effects of C_{spr} and C_{rpr} with respect to the torque and efficiency, respectively, according to the nominal current. Considering the limitations described in figures previous to C_{spr} and C_{rpr} when Figure 14 is examined, the high value of C_{spr} and the low value of C_{rpr} should be selected for high torque. This result is the same as the fixed TAT except for the limitations. When Figure 15 is examined, high values of both C_{spr} and C_{rpr} should be selected for high efficiency by taking into account the limitations that appear. However, these ratios should be selected by taking into consideration torque-efficiency relationship.

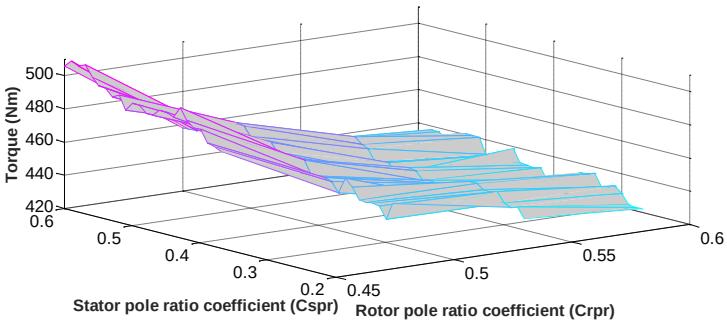

Figure 14. Torque versus pole ratio coefficients

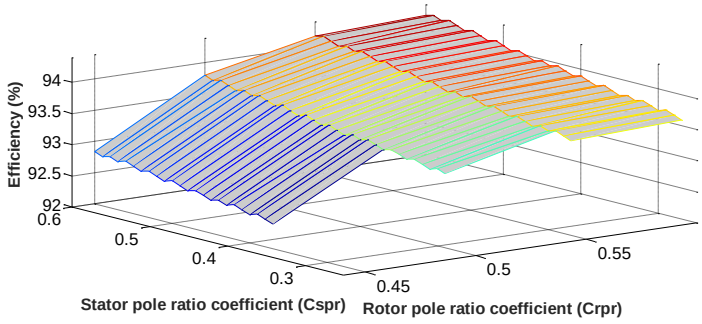

Figure 15. Efficiency versus pole ratio coefficients

4. Conclusions

In this study, the effect of stator and rotor pole ratio coefficients on torque and efficiency have been investigated for two case which constant total ampere-turns and variable total ampere-turns The results obtained for the case which TAT is kept constant are listed as follows.

It has been observed that torque increased as C_{spr} value increased and the torque decreased as C_{rpr} value increased.

As the C_{spr} value increased, the efficiency of ISRM decreased by approximately between 0.3% and 0.95% for fixed TATs. It has been observed that there is a partly change between C_{rpr} values and efficiency efficiency. Because the total ampere- turns did not change and only copper losses have been examined in this study.

The results obtained for the case in which TAT is calculated and for different current variations are listed as follows.

It has been observed that there no exactly linear relationship between C_{spr} values and torque. As the C_{spr} coefficient increased until about 0.55, it has been observed that the torque value increased. However, a negative effect has been observed in the torque after 0.55 value of C_{spr}. It has been observed that the ISRM starts to generate torque after the 0.44 value of C_{rpr} and the torque of ISRM decreased as the ratio increased.

As the C_{spr} value increased, the efficency increased by approximately between 0.5% and 0.8% according to different currents. As the C_{rpr} value increased, the efficiency of ISRM increased by approximately 1.68% for different currents.

In this paper, it is observed that stator and rotor pole ratio coefficients had an effect on the output parameters of the ISRM. Stator and rotor pole ratio coefficients must be taken into account before starting the ISRM design. The effect of stator and rotor pole ratio coefficients on the desired motor performance is presented. As a result, if these coefficients are determined as an optimization problem, it can be stated that appropriate results can be obtained in the torque and efficiency of the ISRM.

5. References

[1] Oshaba, A. S., Ali, E. S., and Elazim, S. A. (2015). ACO based speed control of SRM fed by photovoltaic system. International Journal of Electrical Power & Energy Systems, 67, 529-536.
[2] Zeraoulia, M., Benbouzid, M. E. H., and Diallo, D. (2006). Electric motor drive selection issues for HEV propulsion systems: A comparative study. IEEE Transactions on Vehicular technology, 55(6), 1756-1764.
[3] Yildirim, M., Polat, M., and Kürüm, H. (2014). A survey on comparison of electric motor types and drives used for electric vehicles. In Power Electronics and Motion Control Conference and Exposition (PEMC), 2014 16th International, 218-223
[4] Bose, B. K. (2009). Power electronics and motor drives recent progress and perspective. IEEE Transactions on Industrial Electronics, 56(2), 581-588.
[5] Naayagi, R. T., and Kamaraj, V. (2005). A comparative study of shape optimization of SRM using genetic algorithm and simulated annealing. In Indicon, 2005 Annual IEEE, 596-599
[6] Moreno-Torres, P., Lafoz, M., Blanco, M., Navarro, G., Torres, J., and García-Tabarés, L. (2016). Switched reluctance drives with degraded mode for electric vehicles. In Modeling and Simulation for Electric Vehicle Applications. InTech.
[7] Tursini, M., Villani, M., Fabri, G., and Di Leonardo, L. (2017). A switched-reluctance motor for aerospace application: Design, analysis and results. Electric Power Systems Research, 142, 74-83.
[8] Jakobsen, U., Lu, K., Rasmussen, P. O., Lee, D. H., and Ahn, J. W. (2015). Sensorless control of low-cost single-phase hybrid switched reluctance motor drive. IEEE Transactions on Industry Applications, 51(3), 2381-2387.
[9] Krishnan, R. (2001). Switched reluctance motor drives: modeling, simulation, analysis, design, and applications. CRC press.
[10] Desai, P. C., Krishnamurthy, M., Schofield, N., and Emadi, A. (2010). Novel switched reluctance machine configuration with higher number of rotor poles than stator poles: Concept to implementation. IEEE Transactions on Industrial Electronics, 57(2), 649-659.
[11] Ray, W. F., Lawrenson, P. J., Davis, R. M., Stephenson, J. M., Fulton, N. N., and Blake, R. J. (1986). High-performance switched reluctance brushless drives. IEEE Transactions on Industry Applications, (4), 722-730.
[12] Kosaka, T., Matsui, N., Taniguchi, Y. I., and Do- meki, H. (2000). Some considerations on torque ripple suppression in reluctance motors. Electrical Engineering in Japan, 130(1), 118-128.
[13] Michaelides, A. M., and Pollock, C. (1994). Effect of end core flux on the performance of the switched reluctance motor. IEE Proceedings-Electric Power Applications, 141(6), 308-316.
[14] Nirgude, A., Murali, M., Chaithanya, N., Kulkarni, S., Bhole, V. B., and Patel, S. R. (2016). Nonlinear mathematical modeling and simulation of Switched Reluctance Motor. In Power Electronics, Drives and Energy Systems (PEDES), 2016 IEEE International Conference on, 1-6
[15] Gupta, R. A., Kumar, R., and Bishnoi, S. K. (2010). Modeling and control of nonlinear switched reluctance motor drive. Journal of Electrical Engineering.

[16] Cai, J., Deng, Z., and Liu, Z. (2010). Nonlinear modeling of switched reluctance motor using different methods. In Applied Power Electronics Conference and Exposition (APEC), 2010 Twenty-Fifth Annual IEEE, 1018-1025

[17] Prasad, N., and Jain, S. (2012). Simulation of Switched Reluctance Motor for performance Analysis using MATLAB/SIMULINK Environment and use of FPGA for its control. International Journal of Electrical, Electronics and Computer Engineering, 1(1), 91-98.

[18] Choi, Y. K., Yoon, H. S., and Koh, C. S. (2007). Pole-shape optimization of a switched-reluctance motor for torque ripple reduction. IEEE Transactions on Magnetics, 43(4), 1797-1800.

[19] Arumugam, R., Lindsay, J. F., and Krishnan, R. (1988). Sensitivity of pole arc/pole pitch ratio on switched reluctance motor performance. In Industry Applications Society Annual Meeting, 1988., Conference Record of the 1988 IEEE, 50-54

[20] Güngör, B. A. L., and UYGUN, D. (2010). An approach to obtain an advisable ratio between stator and rotor tooth widths in switched reluctance motors for higher torque and smoother output power profile. Gazi University Journal of Science, 23(4), 457-463.

[21] Omaç, Z., Polat, M., Öksüztepe, E., Yıldırım, M., Yakut, O., Eren, H., Kaya, M., and Kürüm, H. (2018). Design, analysis, and control of in-wheel switched reluctance motor for electric vehicles. Electrical Engineering, 100(2), 865-876.

[22] Kumar, M. K., and Murthy, G. R. K. (2013). Modeling and simulation of 8/6 pole switched reluctance motor with closed loop speed control. In Microelectronics and Electronics (PrimeAsia), 2013 IEEE Asia Pacific Conference on Postgraduate Research in, 89-95